International Journal of Thin Films Science and Technology

http://dx.doi.org/10.18576/ijtfst/070201

Steady State Creep Characteristics of $Sn_{96.5}Ag_{3.5}$ Based Alloys

*M. Y. Salem**

Physics Department, Faculty of Science at New Valley, Assuit University, 72511, El-Kharga, Egypt.

Received: 2 Mar. 2018 Revised: 12 Apr. 2018, Accepted: 17 Apr. 2018.
Published online: 1 May 2018.

Abstract: The creep curves of Sn_{96} $Ag_{3.5}In_{0.5}$, $Sn_{95.5}Ag_{3.5}In_{1.0}$, and $Sn_{95}Ag_{3.5}In_{1.5}$ ternary alloys have been studied at various constant loads from 10 to 19.5 MPa in temperature range from 303 to 393 K. The results indicated that the steady state creep parameters m and steady-state creep rate $\dot{\varepsilon}_{st}$ are increased with increasing both the deformation temperature and the applied stress. Significant improvement in creep of 5% and7% is realized, respectively when compared of the $Sn_{95.5}$ $Ag_{3.5}$ $In_{1.0}$, and Sn_{95} $Ag_{3.5}$ $In_{1.5}$ with Sn_{96} $Ag_{3.5}$ $In_{0.5}$ solder. This finding indicates the capability of newly developed ternary1.5 in solder alloys to serve a much wider array of electronic applications. The activation energies of steady state creep of the alloy have been found to be 27.14 and 30.24, 23.03 and 27.23, 13.13 and 18.32 KJ mol^{-1} in low and high temperature regions for the three ternary alloys, respectively. Therefore, the $Sn_{96}Ag_{3.5}In_{0.5}$ samples showed higher creep resistance (low strain rate) than those with 1.0 In and 1.5 In addition, X- ray diffraction analysis, optical microscope and scanning electron microscopy showed that the formation of stable γ-In Sn_4 IMC could occur and the microstructure is refined with increasing In content.
Keywords: Binary alloy; inter metallic compounds; Steady state creep; Ternary alloys.

1 Introduction

Universal attentions along the ecological effect and health concern of Pb-based solders used in microelectronics lead to the progression of Pb-free solder alternate. Among the lead-free solders, Sn-Ag solder alloy is one of the best candidates, which has been widely used in electronic packaging [1]. For implementation needed fine stabilized solders, an extremely low creep rate is needed. Knowledge of the creep manner of Sn-Ag based solders is one of the best of pre-conditions for utilizing these solders in the industrialization of electronic products; since the sample is aimed for implementation at elevated temperatures. In this case, the time-dependent deformation, i.e. creep mechanisms, play a significant role because of elevation identical temperatures concerned. Furthermore, creep characteristics of the samples are affected by a number of parameters; like phase dimensions, phase morphology, existence of In element as a solid solution in the model or its deposition as Sn-In and grade of ageing [2,3].

Chaouki Sadik et al. [3] established that the creep parameters of the samples based on the chemical component as well as the crystal size and the classification of the Sn-rich phase. Diffusion and dislocation creep, where the load is stringent for choosing the related ratio that each mechanism participates to the comprehensive creep rate $\dot{\varepsilon}$ [4].

$$\dot{\varepsilon}_{total}=\&_{diffusion}+\dot{\varepsilon}_{CG} \quad (1)$$

$$\dot{\varepsilon}=C\sigma^{m} \quad (2)$$

Where; $\dot{\varepsilon}_{CG}$: climb and glide creep rate, C is a constant and m is strain rate sensitivity parameter.

For particular creep technique, deformation mechanism maps (DMMs) display collection of temperature and stress. DMMs are advanced from constituent equations for alloys and are obtained for only a little part of engineering alloys. DMMs show the controlling and energetic creep mechanism for a special temperature and stress. It can also overlie strain rates onto DMMs; it can see how this changes the commanding creep mechanism. Deformation

*Corresponding author E-mail:mahmoudsalem778@gmail.com

mechanisms seem to alter with crystal structure. Rendering single path to design a substance to present elevation creep resistance is to subjoin another phase particle. If the particles intercept grain boundary sliding, they demand lowering the steady state creep rate. Generality creep resistant samples employ this mechanism. Individual crystals are also utilized in coupling with another phase particles. Through creep microstructural variations, dislocations are produced and obliged to transition among the substance making work hardening. Composition of hardening and recovery operation can drive to the construction of sub-grains or dislocation networks.

Effects of creep on microstructure, fracture morphology and inter granular creep ruptures could occur by (i) triple point cracking or (ii) grain boundary cavitation. The operation had been affected by $\varepsilon\cdot$ and testing temperature.

There are different significant elevated temperature phenomena that are linked to creep in expression of the effective deformation modes, such as superplasticity. Superplasticity is the capability of polycrystalline substances to display extremely elevation, and regular elongations before failure. It has been observed that some materials when heated above $0.5T_m$ can elongate to extremely large strains (e.g., ~5000%) [4].

A theory of steady state creep is advanced using Mott's technique of dislocation climb. It is supposed in the dissection that the rate-dominant operation is the propagation of vacancies among dislocations, which are originating vacancies and those which are devastating them. The density of vacancies over a dislocation bar is specified via regulation the variation in the release energy. This gives rise to a higher or lower in the digit of vacancies similar to that of variation in flexible energy that happened through dislocation ascend. The creep formula that consequence from the analysis is [5]:

$$\text{Creep rate} = \text{const}\,(\sigma\alpha/KT)\exp(-Q/KT) \qquad (3)$$

Where α is a stationary (α ~ 3 to 4), Q is the activation energy of self-diffusion, K is Boltzmann's constant, T is absolute temperature, and σ is the stress. This formula is accurate in the stress range from the critical shear stress to a stress around similar to 108 to 109 dynes/cm^2. At high stresses, the $\varepsilon\cdot$ increases further immediately with stress [5]. The relation between steady state creep rate, and grain size was found to be the same, independent of the creep mechanism for the different grain sizes. For specimens with grain diameters above 0.1 mm, the steady state creep rate appeared to be independent of grain size, while for smaller grain diameters, the steady state creep rate increased slightly with decreasing grain size. Strongly textured polycrystalline alloys, which included low angle grain boundaries, showed steady state creep rates that were slightly lower than those observed in randomly oriented polycrystalline copper of the same grain size. The results are explained by considering the contribution of grain boundary shearing to the total strain, and the effect of grain size on the resulting creep substructure [6].

The present paper, therefore, aims to describe the steady state creep behavior of $Sn_{96.5}$-$Ag_{3.5}$ alloy, in which 0.5 In, 1.0 In, and 1.5 In were added to form the respective ternary $Sn_{96}Ag_{3.5}In_{0.5}$, $Sn_{96.5}Ag_{3.5}In_{1.0}$, and $Sn_{95}Ag_{3.5}In_{1.5}$ alloys solder alloy. Using X-ray analysis, Optical Microscopy (OM), Scanning Electron Microscope (SEM), the effect of structure transformation and In-addition on the creep behavior has been discussed.

2 Experimental Procedures

The three solder alloys, $Sn_{96}Ag_{3.5}In_{0.5}$, $Sn_{95.5}Ag_{3.5}In_{1.0}$, and $Sn_{95}Ag_{3.5}In_{1.5}$ alloys were prepared from Sn, Ag, and In (purity 99.99%) by melting. The ingots were drawn to wire samples of diameter 0.8 mm and 50 mm gauge length. The alloy samples were annealed at 453 K for 2 h to eliminate the cold work introduced during swaging, and then slowly cooled to room temperature at a constant cooling rate of $2x10^{-3}$ K/sec. The samples were considered to be completely precipitated [7]. Creep deformations were performed under constant applied stresses from 10 MPa to 19.5 MPa , and tested temperature ranging from 303 to 393 K, in steps of 20 K for the three alloys. The creep tests were carried out in an improved model of creep machine provided with computer [8]. The sensitivity of strain measurement was approximately $\pm 1.0\times10^{-5}$ and the precision of temperature gauge is of the order of ±1 K. A solution of 2% HCl, 3% HNO_3 and 95% (vol.%) ethyl alcohol was used to etch the alloy samples. The creep experiments have been elongated to cover the three intervals of creep regime. The microstructure of the samples was inspected using X-Ray Diffractometer (XRD), and SEM, OM.

3 Results and Discussion

3.1 Features of Creep Curves

The trend in creep curves at all three levels of applied stresses suggests a rapid transition from a short primary creep regime to a steady state and tertiary creep regime. This transion is easier to supervise in the graphs of strain against time that are given in Figs.1 and 2. It can be seen that most curves are characterized by the three characteristic regions: (I) primary, (II) secondary or steady state, and (III) tertiary stage especially at low applied stresses and the others show only two regions primary stage, followed by tertiary stage at higher applied stresses. Since the temperature and stress are stable, the difference in creep rates, $\varepsilon^{\cdot}$, suggests a requisite variation in the internal structure of the sample through time. It should be noted that the whole curves exhibit a distinguished decrease in the creep rate, $\dot{\varepsilon}_{min}$, followed by a regime with a protracted accelerating deformation rate. Never the less, the minimum creep rate, $\dot{\varepsilon}_{min}$, for $Sn_{95}Ag_{3.5}In_{1.5}$ is obtained at higher value of strain (10%) than that for $Sn_{95.5}Ag_{3.5}In_{1.0}$, and Sn_{96} $Ag_{3.5}$ $In_{0.5}$ regardless of the testing temperature. On the other hand, the strain rate and strain to failure are, in General lower for Sn_{96} $Ag_{3.5}$ $In_{0.5}$ samples than for the $Sn_{95.5}$ $Ag_{3.5}$ $In_{1.0}$ and $Sn_{95}Ag_{3.5}In_{1.5}$ samples, in spite of the applied stress are higher in case of the former. This variation in creep attitude perhaps concerned with the variation in the grain size through the samples.

The particular line of creep for the three samples are showed in Fig.1 at 303 K, as strain-time curves at fixed test temperature in the rang from 303 to 393 K with applied stress level in the range of 10.5 to 19.5 MPa. The comparison of creep curves of three alloys are given in Fig.2 at 393 K. The effect of in on $Sn_{96.5}Ag_{3.5}$ lead-free solder alloys is represented in Fig.3, where the creep curves of the alloys are performed at constant stresses of 14.37 MPa. It is obvious that the ternary $Sn_{96}Ag_{3.5}In_{0.5}$ alloy is less in super plasticity than $Sn_{95.5}Ag_{3.5}$-$In_{1.0}$ than and $Sn_{95}Ag_{3.5}In_{1.5}$ solders.

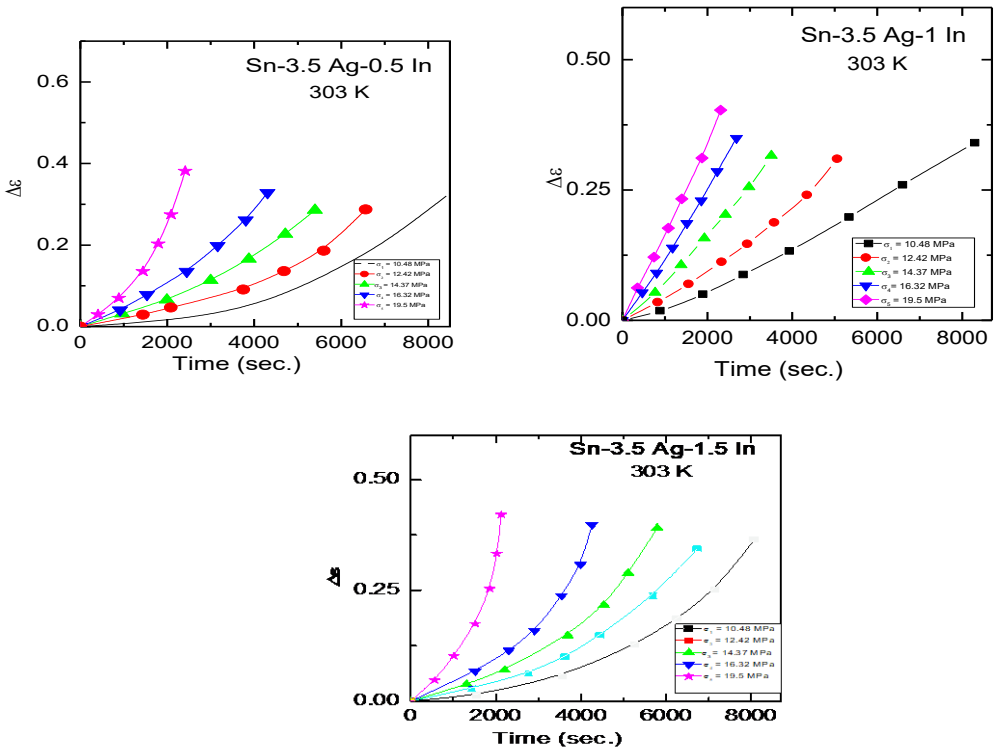

Fig 1. Creep curves at 303 K, and different applied stresses for tested alloys

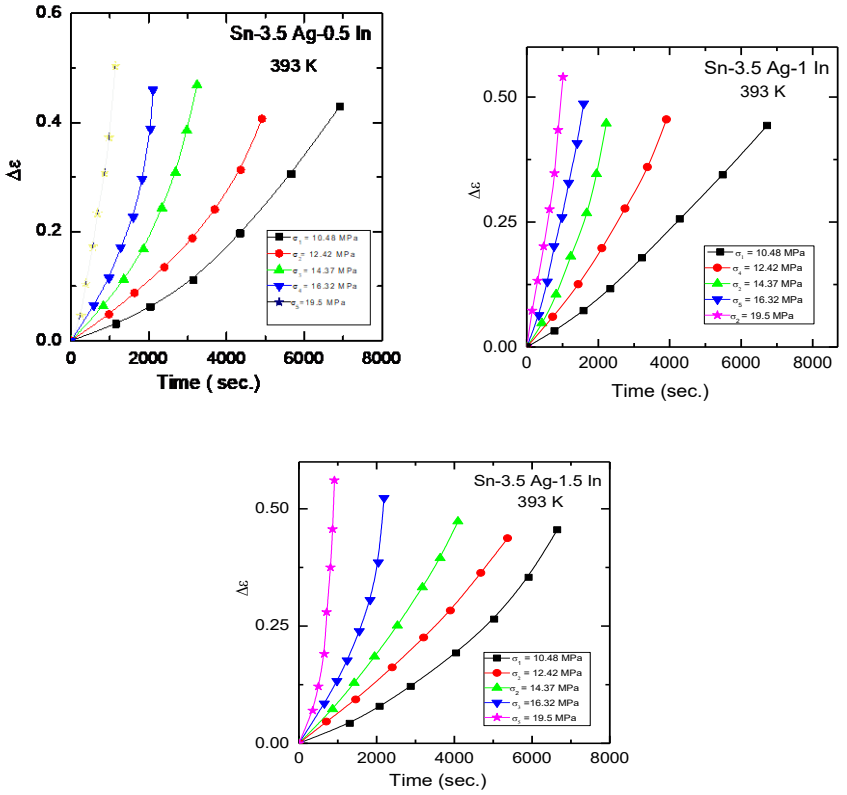

Fig 2. Creep curves at 393 K, and different applied stresses for tested alloys

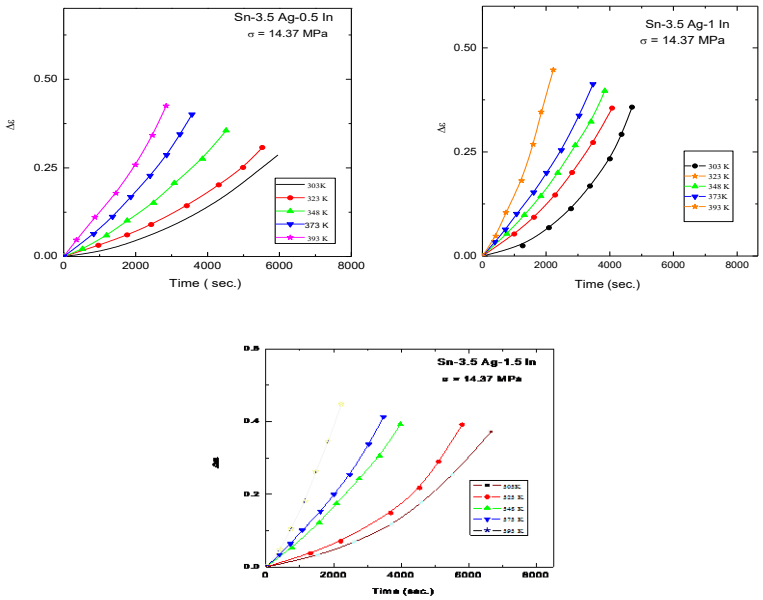

Fig 3. Comparison of isothermal creep curves at constant stress = 14.37 MPa and different temperature.

The steady-state creep rate ε'_{st} is calculated from the slopes of straight lines that related strain with time, as shown in Fig.1,2. It can be seen that the strain rate increases with raising both the temperature and σ (stress). The ε'_{st} values are represented in Table 1. It is shown that the ε'_{st} value is higher for samples $Sn_{95}Ag_{3.5}$ $In_{1.5}$ and intermediate for $Sn_{95.5}$ $Ag_{3.5}In_{1.0}$ and less for $Sn_{96}Ag_{3.5}In_{0.5}$ alloys.

Strain rate sensitivity parameter $m=\partial \ln \sigma/\partial \ln \varepsilon'_{st}$ [8,9,10] was calculated from the slope of the straight lines of lnσ versus $\ln\varepsilon'_{st}$. The activation energy of steady state creep at constant load was determined by using the following equation [3].

$$Q = R\left(\partial \ln \varepsilon_{st} / \partial(1/T)\right) \quad (4)$$

where T and R are the temperature and universal gas constant, respectively. Moreover, the obtained results verify the equation of steady state creep [8, 11,12]

$$\varepsilon'_{st} = c\left(\frac{\sigma}{d}\right)^{1/m} \exp\left(\frac{Q}{kT}\right) \quad (5)$$

Where m = 0.5 for dislocation mounting over grain boundaries [13,14], and d grain size. Therefore, it is considered here that the higher strain is referred to the dislocation motion results in grain boundary sliding (*GBS)* and including it through the deformation creep. The value of *m* was estimated from slopes of straight lines related lnσ with $\ln \varepsilon'_{st}$ as represented in Fig.4. The value of m shown in Table 1, indicating that the sensitivity parameter *m* is temperature dependent.

Table1. Comparison of the steady creep parameters of the tested alloys.

alloys	ε'_{st}	m
$Sn_{96}Ag_{3.5}In_{0.5}$	7.75×10^{-6} : 2.9×10^{-4}	0.27 :0.49
$Sn_{95.5}Ag_{3.5}In_{1.0}$	1.23×10^{-5} : 3.46×10^{-4}	0.3 : 0.55
Sn_{95}-$Ag_{3.5}In_{1.5}$	2.14×10^{-5} : 5.16×10^{-4}	0.4 : 0.74

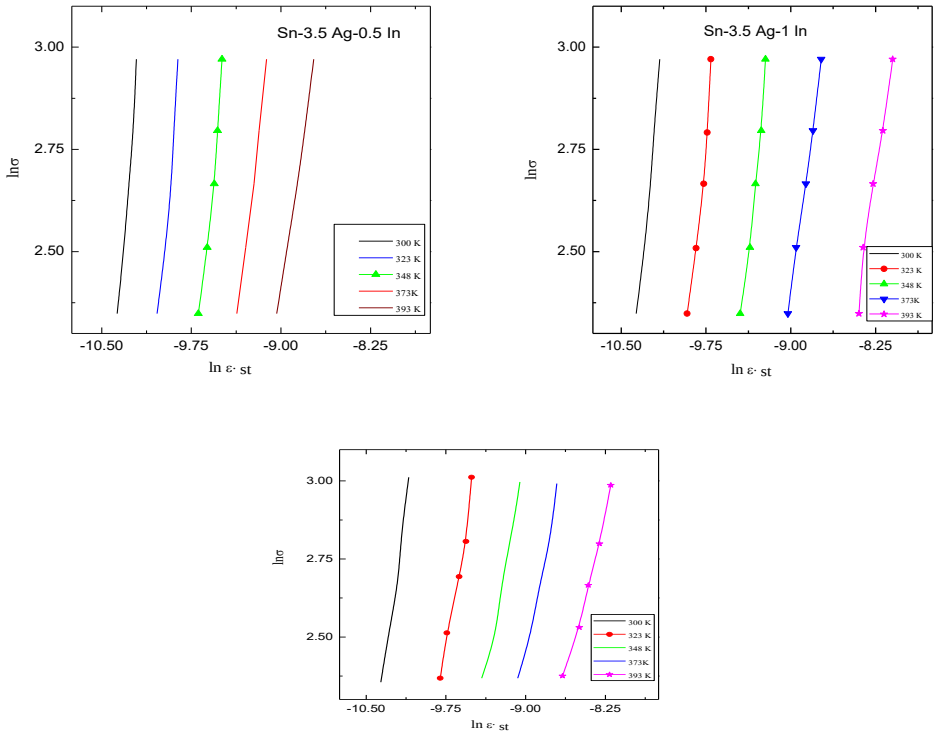

Fig 4. The variation of lnσ with $\ln\varepsilon'_{st}$ for different applied stresses for the three tested ternary alloys.

The steady-state creep rate $\acute{\varepsilon}_{st}$ is plotted versus temperature as shown in Fig.5. The ε'_{st} value of the tested samples is estimated from the gradient of the regular parts of creep curves (Figs.1 and 2). As seen, ε'_{st} increases with increasing the temperature and stress, as presented in Fig.5. The strain rate sensitivity parameter m is found to be increased rapidly with T and stress, as shown in Fig.6.

The activation energy of steady creep at constant loads was estimated using relation (4). The activation energies have been found to be 27.14 and 30.27 KJ/mol for Sn_{96}-$Ag_{3.5}$-$In_{0.5}$ in the low and high temperature regions, respectively (see Fig.7 and 8). Also, the activation energy of $Sn_{95.5}$-$Ag_{3.5}$-$In_{1.0}$, and Sn_{95}-$Ag_{3.5}In_{1.5}$ was estimated and. It is shown that activation energies for Sn_{95}-$Ag_{3.5}$-$In_{1.5}$ alloys are less than those for $Sn_{95.5}$-$Ag_{3.5}$-$In_{1.0}$, and Sn_{96}-$Ag_{3.5}$-$In_{0.5}$ alloys in low and high temperature regions because 1.5In-containing alloy is more refined in grain size and higher super plastic than 1.0 In, and 0.5 In-containing solders.

The activation energies indicated that the steady creep in the low temperature region is dominated by dislocation intersection, while at high temperatures range, is planned by grain boundary sliding [9].

The result for activation energy indicated that the apparent activation energy did not change too much, remaining in the range of 13.16 to27.14 KJ/mol and 18.32 to 30.24 KJ/mol for the three alloys in low and high temperatures regions respectively. The introduction of Ag and In segregation to dislocation cores will form further local lattice distortion around the dislocation lines, and thus the deformation energy required for such crystals will decrease accordingly. However, these Q values have been generally lose to the activation energy reported for dislocation pipe diffusion of β-Sn [15,16].

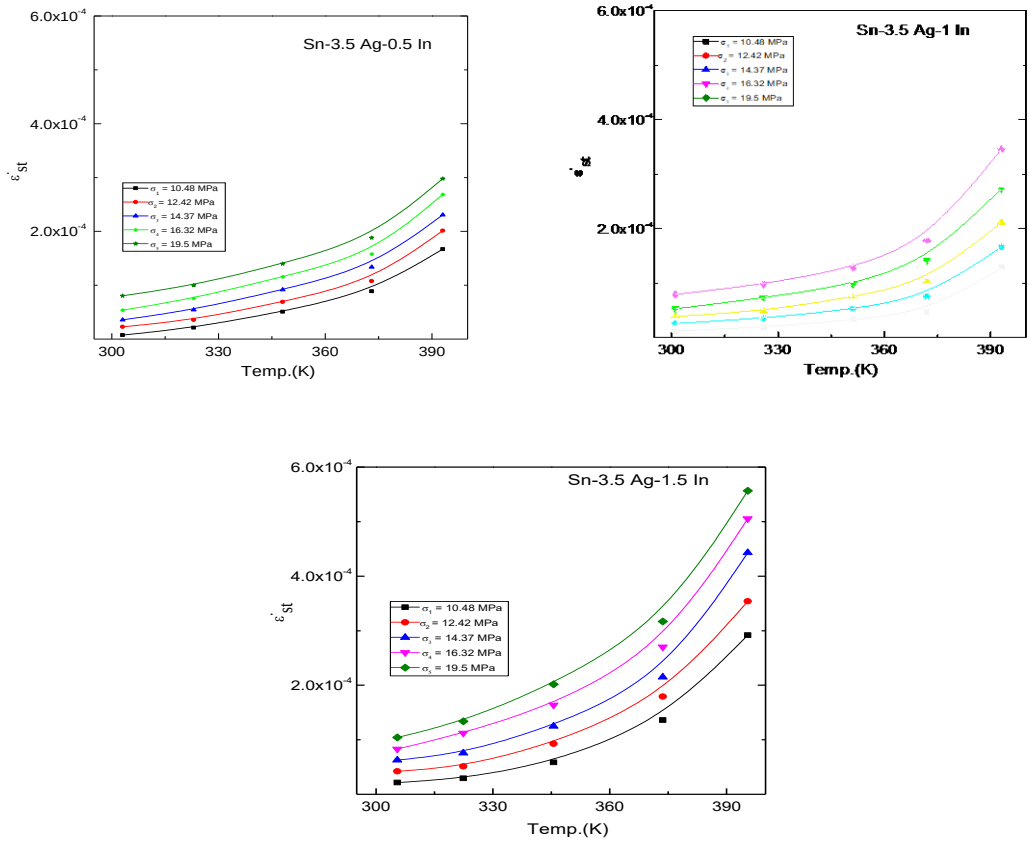

Fig 5. Steady-state strain rate ε'_{st} as a function of creep temperature the tested alloy.

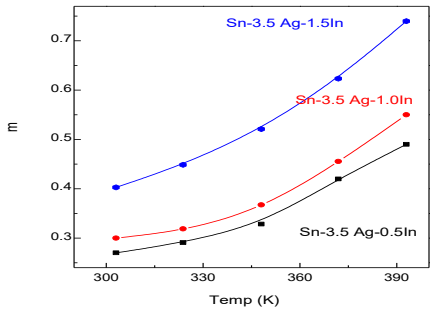

Fig 6. Strain rate sensitivity parameter m as a function of creep temperature for the tested alloys.

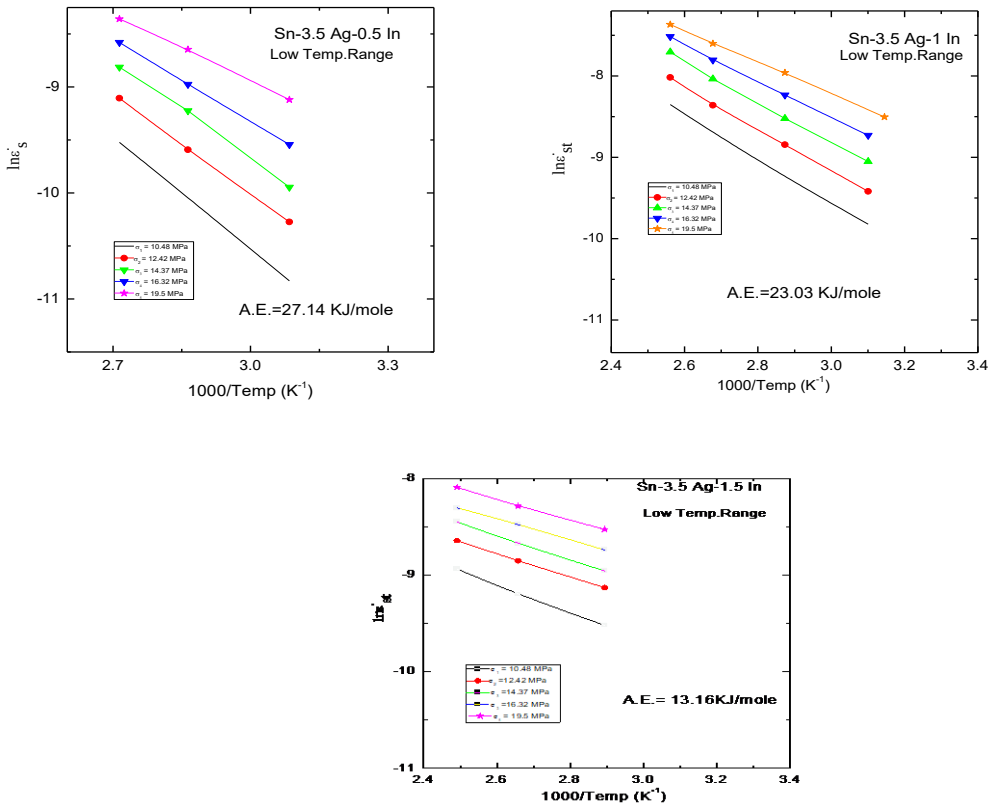

Fig 7. Relation between ln $\varepsilon^{\cdot}_{st}$ and 1000/T at different applied stresses at low temperature.

The relatively higher activation energy of Sn_{95}-$Ag_{3.5}In_{1.5}$ solder suggests that dislocation climb under the influence of the diffusion of In solute atmospheres is the operative deformation mechanism. The variations in Q and m values with the other reported values can be explained by differences in testing methods, microstructure, specimen preparation, measuring errors, and data processing method. As we all know, deformation mechanisms in the particle-strengthened or multi- phase eutectic structures of the Pb-free alloys may thus be similar to those observed in pure tin, but operate at higher stress than in pure Sn [17].

It can be observed in Fig.9a that the microstructure of the $Sn_{96.5}Ag_{3.5}$ binary alloy Consists of relatively fine Ag_3Sn precipitates in The white β-Sn matrix, in addition to eutectic areas. In Fig.9b, the microstructure of the $Sn_{95.5}Ag_{3.5}In_{1.0}$ alloy showed a coarse γ-InSn4, fine Ag_3Sn precipitates in the β-Sn matrix. Fig.9c represented the microstructure of $Sn_{95}Ag_{3.5}In_{1.5}$ alloy, where the volume fraction of γ-$InSn_4$ is increased, in addition to eutectic areas, fine Ag_3Sn, and β-Sn matrix.

The analysis of the X-ray diffraction pattern presented in Fig.10 shows that Sn-Ag-In alloys have β-Sn rich phase and inter metallic compounds of Ag_3Sn phase and γ-$InSn_4$. Fig.11a represented SEM images of the $Sn_{96.5}Ag_{3.5}$ alloy, the microstructure composed of β-Sn areas, fine Ag3Sn precipitates, and eutectic area. In Fig11.b, EDS analysis of the $Sn_{96.5}Ag_{3.5}$ alloys, confirmed the presence of Ag_3Sn.

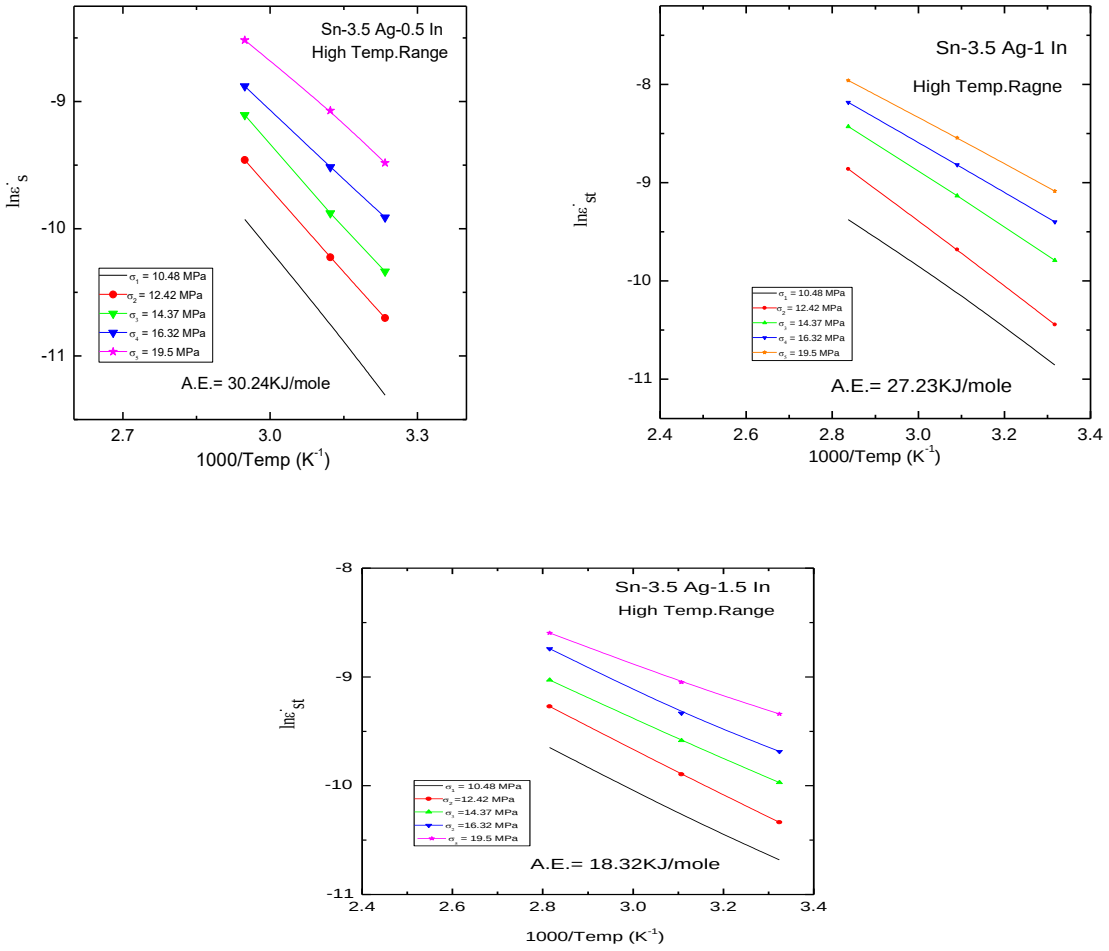

Fig 8. Relation between $ln\dot{\varepsilon}_{st}$ and 1000/T at different applied stresses at high temperature

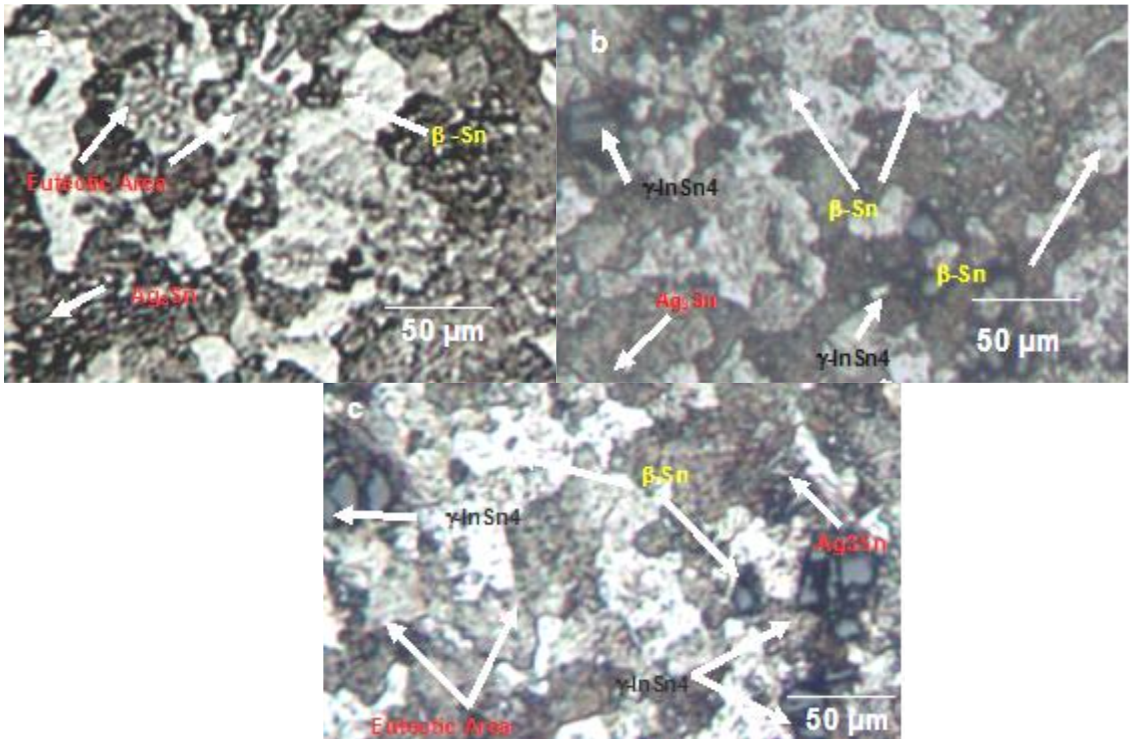

Fig 9. illustrated the OM micostructure a) binary $Sn_{96.5}Ag_{3.5}$, b) $Sn_{95.5}Ag_{3.5}$-$In_{1.0}$ c)) Sn_{95}-$Ag_{3.5}In_{1.5}$

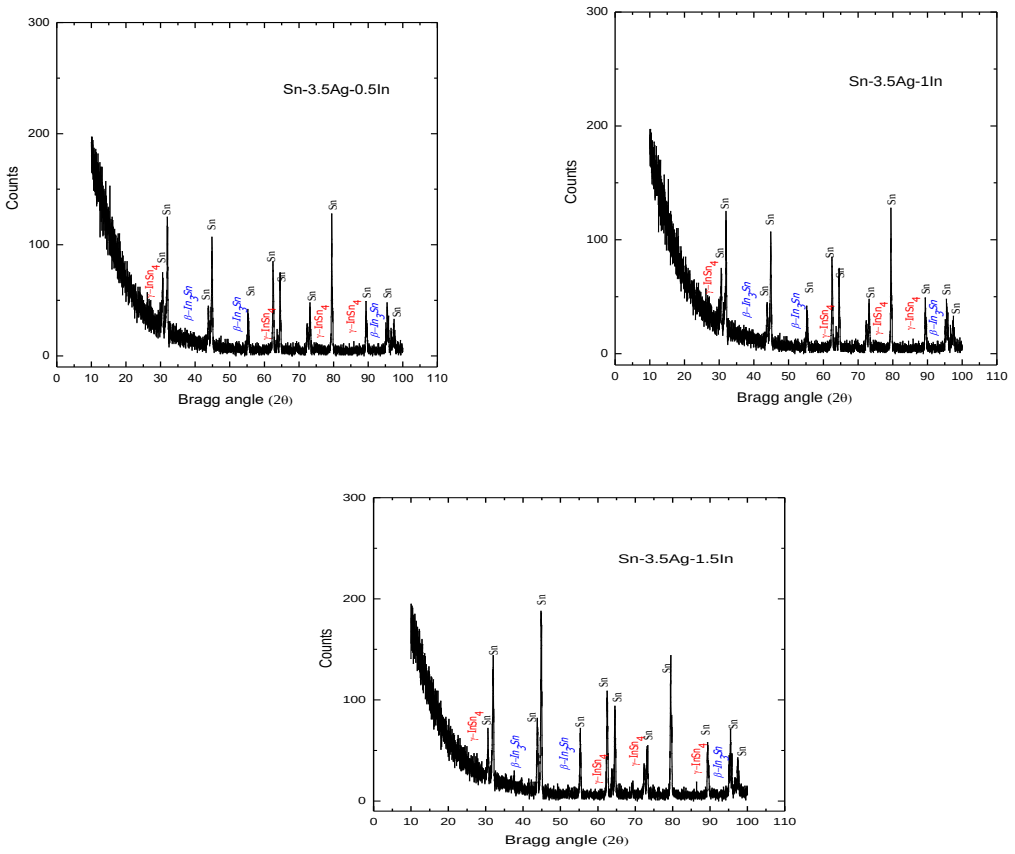

Fig 10. XRD pattern for the three tested ternary alloy showed two phase structure, that is, tetragonal β-Sn rich phase, and the inter metallic compounds as Ag_3Sn, β-In_3Sn and γ-$InSn_4$ phase.

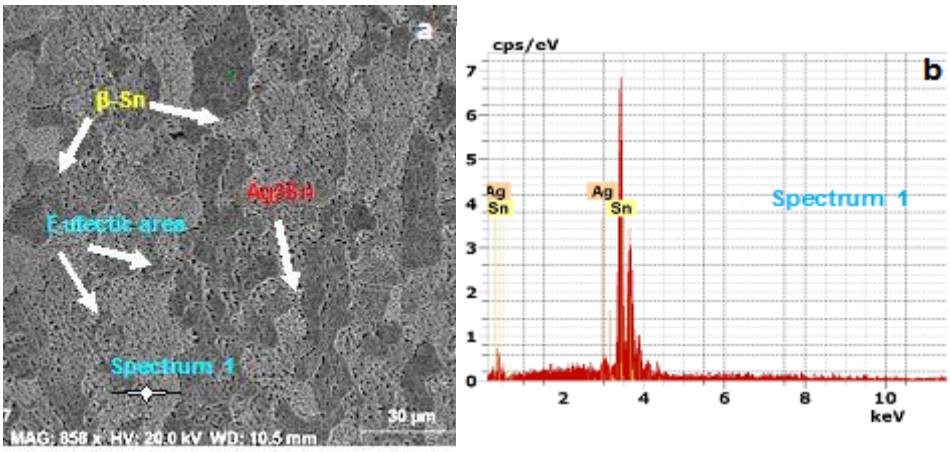

c

Spectrum: Acquisition

El	AN	Series	unn. C [wt.%]	norm. C [wt.%]	Atom. C [at.%]	Error [wt.%]
Sn	50	L-series	90.72	97.75	97.53	2.9
Ag	47	L-series	2.08	2.25	2.47	0.2
		Total:	92.80	100.00	100.00	

Fig 11a. Represented SEM images of the $Sn_{96.5}$-$Ag_{3.5}$ alloys, the microstructure composed of β-Sn areas, fine Ag_3Sn precipitates, and eutectic area. In **Fig11.b**, EDS analysis of the $Sn_{96.5}Ag_{3.5}$ alloys. In **Fig11c**, showed the chemical composition of the $Sn_{96.5}$-$Ag_{3.5}$ alloys.

4 Conclusions

This research has scanned the effect of little addition of In on steady state creep characteristics and microstructure of $Sn_{96.5}$-$Ag_{3.5}$ based alloys. The results are for steady state creep, for all three samples, the activation energies estimated indicate that the activation energies of 0.5In is more than that of 1.0 In and 1.5 In, the result for activation energy indicated that the apparent activation energy did not change too much; these activation energy (Q) values have been generally close to the activation energy reported for dislocation pipe diffusion of β-Sn. Therefore, the 0.5In samples are less elongation than the two other 1.0 In, and 1.5 In. The steady creep parameter m and steady strain rate ε′st raises with raising the deformation temperature and stress. From microstructure examination, relatively fine Ag_3Sn precipitates in the white β-Sn matrix, in addition to eutectic areas, the two $Sn_{95.5}$-$Ag_{3.5}$-$In_{1.0}$ andSn_{95}-$Ag_{3.5}In_{1.5}$ ternary alloys exhibited additional constituent phases of Ag_3Sn IMCs, and γ-$InSn_4$, and eutectic areas. The action of the alloying addition still needs more and more attention.

References

[1] A.A. El-Daly, A.Z. Mohamad ,A. Fawzy,A.M. El-Taher ,Materials Science and Eng., A **528**, 1055-1062, 2011.

[2] Q.S. Zhu, Z.G. Wang, S.D. Wu, J.K. Shang, Mater. Sci. Eng., A **502**, 153-158, 2009.

[3] ChaoukiSadik, Iz-EddineEl Amrani, Abderrahman Albizane., **2(2)**, 83-96, 2014.

[4] M.L. Weaver, Manufacturing Engineering and Technology, Sixth Edition Pearson Education., A, 1-30, 2010.

[5] J. Weertman, Journal of Applied Physics., **26**, 1213, 2004.

[6] M. Herwegh , T. Poulet , A. Karrech , and K Regenauer-Lieb, J. Geophys. Res. Solid Earth., **119**, 900–918, 2014.

[7] M. S. Saker , A. Z. Mohamed etal, Egypt . J. solids B2 ,34(1990). (a)169,(1998)217.

[8] M.Yousf Salem; International Journal of New Horizons in Physics., **4(2)**, 11- 10, 2017.

[9] A.A. El-Daly, A. Fawzy, A.Z.Mohamad, A.M. El-Taher, Journal of Alloys and Compounds., **509**, 4574-4582, 2011.

[10] G. Saada, S.A. Fayekb, A. Fawzya, H.N.Solimana, Gh.Mohammeda, Materials Science and Engineering., **A 527**, 904-910, 2010.

[11] A.A. El-Daly, A.M. Abdel-Daiem, M. Yousf, Materials

Chemistry and Physics.,**74**, 43-51,2002.

[12] A. Fawzy, S.A.Fayek, M.Sobhy, E.Nassr, M.M. Mousa, G. Saad, J Mater Sci, Mater Electron., **24**, 3217, 2013.

[13] A.A. El-Dalya, A.Z. Mohamad, A. Fawzy, A.M.El-Taher, Materials Science and Engineering., A**528**, 1055-1062, 2011.

[14] A.A. El-Daly, A.M. El-Taher, Materials Science and Design., **47**, 607-613,2013.

[15] Mahmudi R, Geranmayeh AR, Noori H, Shahabi M. Impression creep of hypoeutectic Sn–Zn lead-free solder alloys. Mater Sci Eng., A**6**, 491-110, 2008.

[16] Geranmayeh AR, Nayyeri G, Mahmudi R. Microstructure and impression creep behavior of lead-free Sn–5Sb solder alloy containing Bi and Ag. Mater Sci Eng., A**9**, 547-110, 2012.

[17] A.A. El-Daly, A.E. Hammad, G.A. Al-Ganainy, and A.A. Ibrahiem; Enhancing mechanical response of hypoeutectic Sn–6.5Zn solder alloy using Ni and Sb additions; Materials Science and Design., **52**, 966-973, 2013.